

## Prediction model of crowd noise in large waiting halls

Hongshan Liu, Hui Ma, Chao Wang, et al.

Citation: [The Journal of the Acoustical Society of America](#) **152**, 2001 (2022); doi: 10.1121/10.0014347

View online: <https://doi.org/10.1121/10.0014347>

View Table of Contents: <https://asa.scitation.org/toc/jas/152/4>

Published by the [Acoustical Society of America](#)

---

### ARTICLES YOU MAY BE INTERESTED IN

[A time series analysis model of the relationship between psychoacoustic parameters of urban soundscape spatial sequences and emotional changes](#)

[The Journal of the Acoustical Society of America](#) **152**, 2022 (2022); <https://doi.org/10.1121/10.0014287>

[Rayleigh limit extended: Scattering from a fluid sphere](#)

[The Journal of the Acoustical Society of America](#) **152**, R7 (2022); <https://doi.org/10.1121/10.0014345>

[Intelligibility and detectability of speech measured diotically and dichotically in groups of listeners with, at most, "slight" hearing loss](#)

[The Journal of the Acoustical Society of America](#) **152**, 2013 (2022); <https://doi.org/10.1121/10.0014419>

[Acoustic scattering and the exact Green function](#)

[The Journal of the Acoustical Society of America](#) **152**, 2038 (2022); <https://doi.org/10.1121/10.0014346>

### REVIEWS OF ACOUSTICAL PATENTS

[The Journal of the Acoustical Society of America](#) **152**, 1995 (2022); <https://doi.org/10.1121/10.0014344>

[The ACOUCOU platform: Online acoustic education developed by an interdisciplinary team](#)

[The Journal of the Acoustical Society of America](#) **152**, 1922 (2022); <https://doi.org/10.1121/10.0014170>

---





**Advance your science and career  
as a member of the**

**ACOUSTICAL SOCIETY OF AMERICA**

LEARN MORE



## Prediction model of crowd noise in large waiting halls

Hongshan Liu, Hui Ma, Chao Wang,<sup>a)</sup>  and Jian Kang<sup>b)</sup> 

School of Architecture, Tianjin University, Tianjin, 300072, China

### ABSTRACT:

Crowd noise is usually the primary noise in large waiting halls, and it is difficult to predict because it is influenced by several factors such as room acoustics and crowd characteristics. This study developed a crowd noise prediction model based on the superposition of direct and reverberant sound energy using the factors of the spatial layout of waiting halls, number and distribution of crowds, behavior ratio (ratio of vocal passengers to the total number of passengers), and average crowd sound power. To verify the model, on-site measurements were conducted in two large waiting halls to obtain the necessary input parameters. The crowd noise levels in one of the waiting halls were obtained from 1-s noise level data after excluding broadcast periods. A method for determining an individual's average sound power based on the model was also presented and found to be approximately 70.6 dB. Finally, the model was verified using measured data, and it showed that the model could accurately predict the average crowd noise level and changing trend of crowd noise in temporal and spatial dimensions with an average  $R$ -square of approximately 0.55 and average difference of approximately 1.1 dBA between the predicted and measured results.

© 2022 Acoustical Society of America. <https://doi.org/10.1121/10.0014347>

(Received 6 July 2022; revised 9 September 2022; accepted 12 September 2022; published online 3 October 2022)

[Editor: Manuj Yadav]

Pages: 2001–2012

### I. INTRODUCTION

A significant number of huge transportation hubs are being constructed as critical transport infrastructure worldwide. In China, the maximum number of passengers gathered in the waiting hall in a large railway station can be over 3000.<sup>1</sup> However, there is usually a high level of noise and poor speech intelligibility in large waiting halls.<sup>2–5</sup> Crowd noise is one of the most important noise sources<sup>3</sup> and influenced by the surrounding environment and crowd characteristics.<sup>6</sup> Thus, it exhibits significant fluctuations in the temporal and spatial dimensions. However, present studies on crowd noise in large waiting halls have mostly focused on the average noise level and subjective evaluation of the crowd.<sup>3,7–10</sup> The relationship between the fluctuations and aforementioned influencing factors has not been investigated and modeled. Hence, the purpose of this study is to develop a prediction model of crowd noise based on crowd distribution and the law of sound energy superposition in a large waiting hall to help in the development of a more targeted acoustic design.

In general, two steps are required to develop a prediction model for crowd noise: (1) determination of the average crowd sound power and (2) establishment of sound energy superposition rules for multiple sound sources. There are typically two methods for determining the average crowd sound power. One method is to measure the sound power of human speech in a laboratory.<sup>11</sup> However, this method

suffers from test environment distortion because the sound power is influenced by several factors such as the surrounding environment, feedback effect of noise on speech sound power (the Lombard effect),<sup>12,13</sup> and the gender, age, group size, or speaking ratio of the crowd.<sup>6,14</sup> The other method is to infer the sound power based on the crowd noise level in space using the spatial propagation pattern of the noise, and this method is actually the inverse process of noise prediction. Hodgson *et al.*<sup>15</sup> used this method to calculate the average speech sound power and Lombard effect in canteens, but only the reverberant sound energy was considered. Wang *et al.*<sup>16</sup> proposed a model for calculating speech sound power based on this method, which accounts for both direct and reverberant sound energy based on the uniform distribution and fixed spacing of dining crowds in university canteens. However, the results can easily be overfitted and offer a deceptive impression of high accuracy because the training and test sets of the noise data are not well separated.

The following stage is to model the sound energy superposition rules for sound sources based on the acoustic properties of space. Several studies have developed crowd noise prediction models for public spaces such as restaurants and bars. Hodgson *et al.*<sup>17</sup> measured the sound pressure levels of different sources in 11 university classrooms and established an empirical prediction formula for sound pressure levels using multiple linear regression. Hodgson *et al.*<sup>15</sup> then measured the noise levels in ten restaurants and developed a crowd noise prediction model based on diffuse sound field theory that incorporated factors, such as the number of people, group size, and Lombard effect, and optimized these unknown parameters using iterative algorithms. Navarro and Pimentel<sup>18</sup> evaluated the noise levels in two canteens

<sup>a)</sup>Electronic mail: pdwangchao@tju.edu.cn

<sup>b)</sup>Also at: University College London (UCL) Institute for Environmental Design and Engineering, The Bartlett, UCL, Central House, 14 Upper Woburn Place, London WC1H 0NN, UK.

using a model based on diffuse sound field theory and proposed a maximum A-weighted sound pressure level evaluation value. Rindel<sup>19,20</sup> constructed a noise prediction model based on the diffuse sound field assumption and compared its predicted results with the onsite measured noise levels to optimize the Lombard slope and group size. It can be seen that the models proposed in the previous studies focus entirely on the superposition of reverberant sound energy with no consideration of the effect of direct sound on crowd noise level. However, Connor<sup>21</sup> pointed out that a crowd noise prediction model must account for direct and reverberant sound energy, whereas one type of sound energy might predominate in some circumstances. Nijs *et al.*<sup>22</sup> evaluated the effect of direct sound energy on crowd noise and found that direct sound had a significant effect on the noise levels of sound fields with high absorption coefficients and lacking reflected sound, which is common in extra-large spaces that exhibit non-diffuse sound field characteristics.<sup>2</sup> Hodgson<sup>23,24</sup> pointed out that as the non-diffusivity of space increases, traditional sound pressure level prediction formulas tend to overestimate the sound pressure level far from a source because of the rapid decay of reverberant energy with distance. Therefore, the superposition of the direct sound energy is particularly important for the prediction of noise levels in extra-large spaces. Exploring the superposition pattern of direct nonsound energy requires additional consideration of the spatial distribution of crowds, crowd spacing, and other parameters. Tang *et al.*<sup>25</sup> developed a crowd noise prediction model that incorporates the number and distribution of people, distance between people, Lombard effect, and crowd absorption factors based on the assumption that crowds are evenly distributed in a two-dimensional lattice. However, the crowd distribution in a waiting hall depends on the location of the seating areas, which is different from the assumed concept of crowds increasing from the perimeter or core of the canteen. Furthermore, the direct sound energy of each person is superimposed individually according to the spatial location of crowds in Tang's model, which leads to a large amount of computation and reduces the ease of use and convenience of

the model. Therefore, the goal of this study is to use a simple mathematical model to describe the superposition law of the direct acoustic energy in waiting halls.

In this study, a prediction model based on direct and reverberant sound energy superposition was established to consider the layout of the waiting hall, location of the crowd, and distance between passengers in a large waiting hall. Subsequently, on-site measurements were conducted throughout the day in two waiting halls to determine ambient and crowd noise, behavior categories and ratios, and average crowd sound power. Finally, the prediction model was evaluated using previously presented data. The detailed framework of this study is illustrated in Fig. 1.

## II. CROWD NOISE PREDICTION MODEL

Considering that the distribution of crowds in large waiting halls varies from area to area, the partitioning of the total calculation area can obtain outcomes that are closer to the real situation, thus, improving the accuracy of the prediction. The following plane division method was proposed after on-site observations in the waiting hall. The waiting hall's plan area can be roughly divided into a seating area and traffic area according to the function. Passengers in the seating area were densely and evenly distributed often with fixed positions and spacing (the majority of crowds in the waiting hall were concentrated in the seating area, as shown in Sec. IV B). In contrast, there were relatively fewer passengers in the traffic areas, and they were randomly located. Based on the above analysis, the full prediction model was first split into two parts, the seating area and traffic area, as shown in Fig. 2.

### A. Seating area for crowds

First, a superposition model for direct sound energy was constructed, where the sound energy superposition was calculated using the assumption of a uniform distribution of passengers and integration calculations. The following superposition model is based on a special case in which the

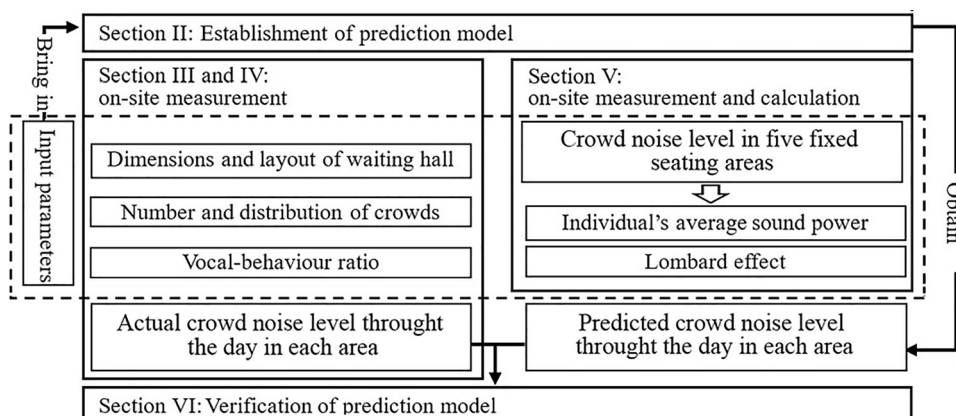


FIG. 1. The research framework.

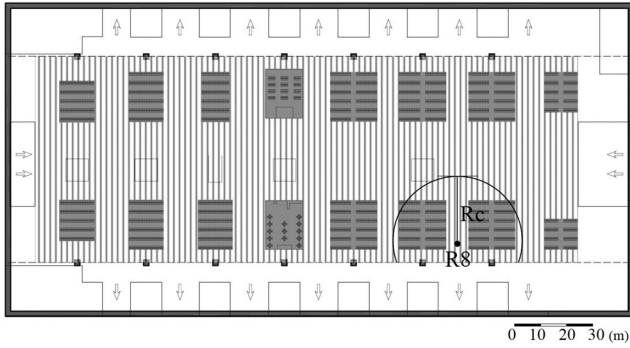


FIG. 2. The partitioning of the waiting hall plan in which the gray parts are the seating areas and the vertical line parts are the traffic areas.

receiver is located at a corner of the seating area. Considering a single seating area as an example, a coordinate system was built with the receiver (coordinate origin) positioned at the corner of the seating area, as illustrated in Fig. 3. Assuming that the lengths of the seating area's long and short sides were  $l$  (m) and  $w$  (m), respectively, and the crowd spacing (distance between adjacent passengers) was  $m$  (m), the behavior ratio was  $\alpha_{\text{behavior ratio}}$ , which was the ratio of the number of active passengers (people who make noise, including speech and activity) to the total number of passengers at a given moment, then the total number of active passengers  $N$  in the seating area is

$$N = \frac{lw}{m^2} \alpha_{\text{behavior ratio}} \tag{1}$$

Assuming an infinitesimal element  $dldw$  exists in the seating area, as shown in Fig. 3, the number of passengers in the infinitesimal element,  $dN$ , is

$$dN = \frac{dldw}{m^2} \alpha_{\text{behavior ratio}} \tag{2}$$

Suppose that the average sound power of a passenger at coordinates  $(l, w)$  is  $W_p(W)$ , and its sound intensity generated at a distance,  $r_0(m)$ , is  $I_0 (W/m^2)$ , the sound intensity emitted by this passenger at the receiver is

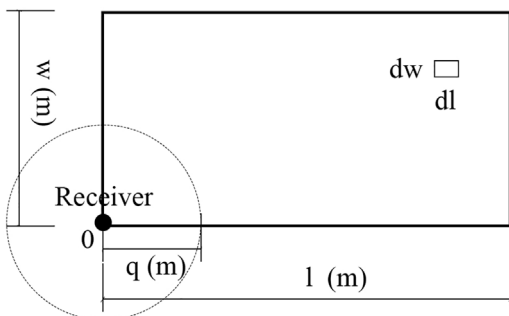


FIG. 3. The coordinate system of the seating area.

$$I_r = \frac{I_0 r_0^2}{l^2 + w^2} \tag{3}$$

The sound intensity emitted by this passenger is divided equally among all of the infinitesimal elements in the area occupied by the passenger. The sound intensity emitted by an infinitesimal element at the receiver is

$$\delta I = dN I_r = \frac{I_0 r_0^2}{(l^2 + w^2) m^2} \alpha_{\text{behavior ratio}} dl dw \tag{4}$$

Because there existed a minimal distance between passengers in reality, noise sources closer than  $q$  (m) from the receiver were excluded to avoid the occurrence of excessive values, as illustrated in Fig. 3. The total sound intensity generated by the entire seating area at the receiver is

$$I = \frac{I_0 r_0^2}{m^2} \alpha_{\text{behavior ratio}} \int_q^l \int_q^w \frac{1}{(l^2 + w^2)} dl dw \tag{5}$$

Because of the lack of an elementary function expression for the results of the double integral with a rectangular integral region and the fact that the results could only be approximated by the computer's numerical integration method, the integral region was simplified to a circle and square with the same area.

- (a) Circle: The radius of the circle corresponding to the rectangular area is  $R = \sqrt{(lw)/\pi}$ , and Eq. (5) is simplified as

$$I = \frac{2\pi I_0 r_0^2}{m^2} \alpha_{\text{behavior ratio}} \int_q^R \frac{1}{r} dr \tag{6}$$

The integral result is

$$I = \frac{2\pi I_0 r_0^2}{m^2} \alpha_{\text{behavior ratio}} \ln \frac{R}{q} \tag{7}$$

An important limitation of the circle simplification is that the receiver can only be located in the center of the area.

- (b) Square: The side length of the square corresponding to the rectangular area,  $b = \sqrt{lw}$ , then Eq. (5) is simplified to

$$I = \frac{I_0 r_0^2}{m^2} \alpha_{\text{behavior ratio}} \int_q^b \int_q^b \frac{1}{(l^2 + w^2)} dl dw \tag{8}$$

Conversion to the polar coordinate system is done for the purpose of performing integral calculations such that

$$I = \frac{I_0 r_0^2}{m^2} \alpha_{\text{behavior ratio}} \left[ \int_q^b \frac{1}{r^2} \left( \int_0^{\pi/2} d\theta \right) r dr + \int_b^{\sqrt{2b^2}} \frac{1}{r^2} \left( \int_{\arccos b/r}^{\arcsin b/r} d\theta \right) r dr \right] \tag{9}$$

The integral result is

$$I = \frac{I_0 r_0^2 \alpha_{\text{behavior ratio}}}{2m^2} [\pi \ln^{b/q} + (\pi \ln^2 - 2G)] \approx \frac{I_0 r_0^2 \alpha_{\text{behavior ratio}}}{2m^2} [\pi \ln^{b/q} + 0.35], \quad (10)$$

where  $G = \sum_{n=0}^{\infty} (-1)^n / (2n + 1)^2$  is the Cartland constant, which can take a limit value of 0.9159 when  $n \rightarrow \infty$ .

When the receiver is located inside or outside of the target seating area, the sound energy superposition model can be obtained by adding or subtracting the sound energy from different areas using the following zoning method, as shown in Fig. 4.

The conversion of the sound intensity at the receiver into the sound pressure level can be derived directly from the following procedure. According to the law that the sound pressure level is approximately equal to the sound intensity level in air, the formula for calculating sound pressure level could be expressed as (taking the circle simplification as an example)

$$\begin{aligned} \text{SPL}_{\text{seating,dir}} \approx L_I &= 10 \lg \frac{I}{I_s} \\ &= 10 \lg \left( \frac{I_0 r_0^2}{I_s} \right) + 10 \lg \left( \frac{2\pi}{m^2} \ln \frac{R}{q} \right) \\ &\quad + 10 \lg \alpha_{\text{behavior ratio}}. \end{aligned} \quad (11)$$

The first term in Eq. (11) is

$$10 \lg \left( \frac{I_0 r_0^2}{I_s} \right) = 10 \lg \left( \frac{4\pi I_0 r_0^2}{I_s} \frac{1}{4\pi} \right) = L_w - 11, \quad (12)$$

then there is

$$\text{SPL}_{\text{seating,dir}} = L_w + 10 \lg \left( \frac{2\pi}{m^2} \ln \frac{R}{q} \right) - 11 + 10 \lg \alpha_{\text{behavior ratio}}. \quad (13)$$

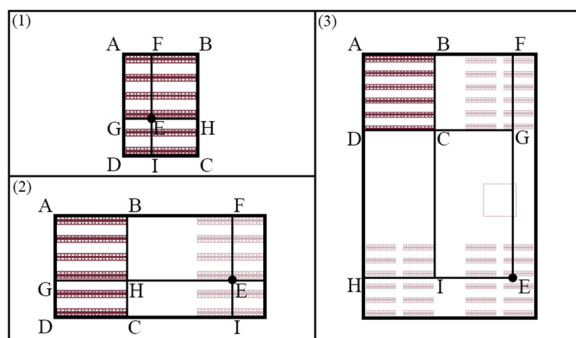


FIG. 4. (Color online) The sound energy superposition of crowd noise when the receiver was located inside or outside the target seating area. (1) Inside, receiver E:  $I_{ABCD} = I_{EGAF} + I_{EFBH} + I_{EIDG} + I_{EHCI}$ ; (2) outside, the seating area and receiver E in the same row or column:  $I_{ABCD} = I_{EGAF} + I_{EIDG} - I_{EIBF} - I_{EICH}$ ; and (3) outside, the seating area and receiver I in different rows or columns:  $I_{ABCD} = I_{EHAF} - I_{EIBF} - I_{EHDG} + I_{EICG}$ .

The square simplification result is

$$\begin{aligned} \text{SPL}_{\text{seating,dir}} &= L_w + 10 \lg \left[ \frac{\pi}{2m^2} \ln^{b/q} + \frac{1}{2m^2} (0.35) \right] \\ &\quad - 11 + 10 \lg \alpha_{\text{behavior ratio}}. \end{aligned} \quad (14)$$

Equation (14) is used to calculate the direct crowd noise level, and the reverberant crowd noise level is calculated using the traditional sound pressure level formula,

$$\text{SPL}_{\text{seating,rev}} = L_w + 10 \lg \frac{4}{R} + 10 \lg (N_{\text{total}} \alpha_{\text{behavior ratio}}), \quad (15)$$

where  $N_{\text{total}}$  is the total number of passengers in the seating area.

The total crowd noise level of the seating area is

$$\text{SPL}_{\text{seating,tot}} = 10 \lg (10^{\text{SPL}_{\text{seating,dir}}/10} + 10^{\text{SPL}_{\text{seating,rev}}/10}). \quad (16)$$

(a) The total crowd noise level for the circle simplification is

$$\begin{aligned} \text{SPL}_{\text{seating,tot}} &= L_w + 10 \lg \left[ \left[ \frac{2\pi}{m^2} \ln \frac{R}{q} \right] + 10^{1.1} \frac{4}{R} N_{\text{total}} \right] \\ &\quad - 11 + 10 \lg \alpha_{\text{behavior ratio}}. \end{aligned} \quad (17)$$

(b) The total crowd noise level for the square simplification is

$$\begin{aligned} \text{SPL}_{\text{seating,tot}} &= L_w + 10 \lg \left[ \left[ \frac{\pi}{2m^2} \ln^{b/q} + \frac{1}{2m^2} (0.35) \right] \right. \\ &\quad \left. + 10^{1.1} \frac{4}{R} N_{\text{total}} \right] - 11 + 10 \lg \alpha_{\text{behavior ratio}}. \end{aligned} \quad (18)$$

## B. Traffic area for crowds

The random distribution of crowds within the traffic area resulted in varying crowd-to-receiver distances and considering the distance elements individually would greatly increase the computational effort. Therefore, the traffic area was first divided into two parts based on the concept of reverberation radius,  $R_c$ ,<sup>18</sup> as shown in Fig. 2. Taking receiver R8 as an example, passengers in the circular area were within the reverberation radius, and those in the rest of the vertical line area were outside of the reverberation radius.

Assuming that the traffic area within the reverberation radius accounts for  $B$  of the total traffic area, then the area outside of the reverberation radius accounts for  $1 - B$ . The total number of passengers in the traffic area is  $N_{\text{traffic}}$ , and the number of passengers inside ( $N_{\text{traffic},1}$ ) and outside ( $N_{\text{traffic},2}$ ) of the reverberation radius are

$$N_{\text{traffic},1} = N_{\text{traffic}} B, \quad N_{\text{traffic},2} = N_{\text{traffic}} (1 - B). \quad (19)$$

The noise level of the passengers in the traffic area within the reverberation radius is calculated using the traditional sound pressure level formula,

$$SPL_{\text{traffic},1} = L_w + 10 \lg \left( \frac{Q}{4\pi r_m^2} + \frac{4}{R} \right) + 10 \lg N_{\text{traffic},1}, \quad (20)$$

where the distance element,  $r_m$ , is the average distance from the crowds to the receiver within the reverberation radius based on the random distribution of the crowds,  $2\pi r_m^2 = \pi R_c^2$ .  $Q$  is the directivity factor of the sound source and has been assumed to be one or two.<sup>15,16,18,19,25</sup> Rindel<sup>19</sup> and Hodgson<sup>15</sup> used  $Q=2$  for calculating the voice output level at 1 m ahead of a single source. Wang *et al.*,<sup>16</sup> Navarro and Pimentel,<sup>18</sup> and Tang *et al.*<sup>25</sup> used  $Q=1$  to predict crowd noise, considering the random distribution of the crowd in the canteen. The passengers in the traffic area of the waiting hall are also randomly distributed and, therefore,  $Q=1$  is used in the subsequent calculations.

For the noise level of passengers in the traffic area outside of the reverberation radius, only the reverberant sound energy is considered such that

$$SPL_{\text{traffic},2} = L_w + 10 \lg \left( \frac{4}{R} \right) + 10 \lg N_{\text{traffic},2}. \quad (21)$$

The waiting hall volume is  $V$  ( $\text{m}^3$ ), its internal surface area is  $S$  ( $\text{m}^2$ ), and its reverberation radius,  $R_c$  (m), is as follows:<sup>25,26</sup>

$$R_c = 0.14 \sqrt{Q \frac{S\alpha}{1-\alpha}}, \quad (22)$$

$$\alpha = \frac{A_{\text{total}}}{S} = \frac{\alpha_{\text{space}}S + \alpha_{\text{person}}N + 4MV}{S}, \quad (23)$$

where  $A_{\text{total}}$  is the total spatial sound absorption,  $\alpha_{\text{space}}$  is the average absorption coefficient of the interior surface of a waiting hall without passengers,  $\alpha_{\text{person}}$  is the absorption coefficient per passenger, and  $4MV$  is the air absorption.

The total crowd noise at the receiver is composed of the above three components:

$$SPL_{\text{total}} = SPL_{\text{seating}} \ddagger SPL_{\text{traffic},1} \ddagger SPL_{\text{traffic},2}, \quad (24)$$

where  $\ddagger$  indicates decibel addition. This formula is the crowd noise prediction model and contains the following

parameters: the average crowd sound power (including the Lombard effect), the layout of the waiting hall, size of the seating area, number of passengers and their spatial distribution, and behavior ratio. Appropriate settings for these parameters and whether reverberant sound energy makes a significant contribution to crowd noise in large waiting halls will be examined in further detail in Sec. VI.

### III. ON-SITE MEASUREMENT

According to the prediction model in Sec. II, the main objective of the on-site measurement is to obtain the following parameters: dimensions and layout of the waiting hall, number and distribution of crowds, vocal-behavior categories, and ratio. The noise level in the waiting hall is measured to verify the accuracy of the prediction model.

#### A. Measurement site

On-site measurements were conducted at the Shenyang and Changchun railway stations because of their favorable transportation locations and high passenger carrying capacities. The actual photos and the spatial layouts of the two waiting halls are shown in Figs. 5 and 6, respectively, and the plan dimensions and other parameters are listed in Table I.

#### B. Procedure of measurements

Noise level measurements, counting of passenger numbers, and behavior categories were carried out in each waiting hall. The test period lasted from 4:20 a.m. to 10:30 p.m., which corresponded to the typical operating hours of the waiting hall during the non-Spring Festival travel period. During the test, the air conditioning system was switched on, the room temperature was approximately 16 °C, and the air humidity was approximately 30%.

##### (1) Noise level

- (a) Twenty measuring points were arranged in each of the two waiting halls as shown in Fig. 6. To obtain more noise data with limited test costs, the 20 measuring points were divided into 5 groups (group 1, R1–R4; group 2, R5–R8; group 3,



(a)



(b)

FIG. 5. (Color online) Photographs of the two waiting halls.

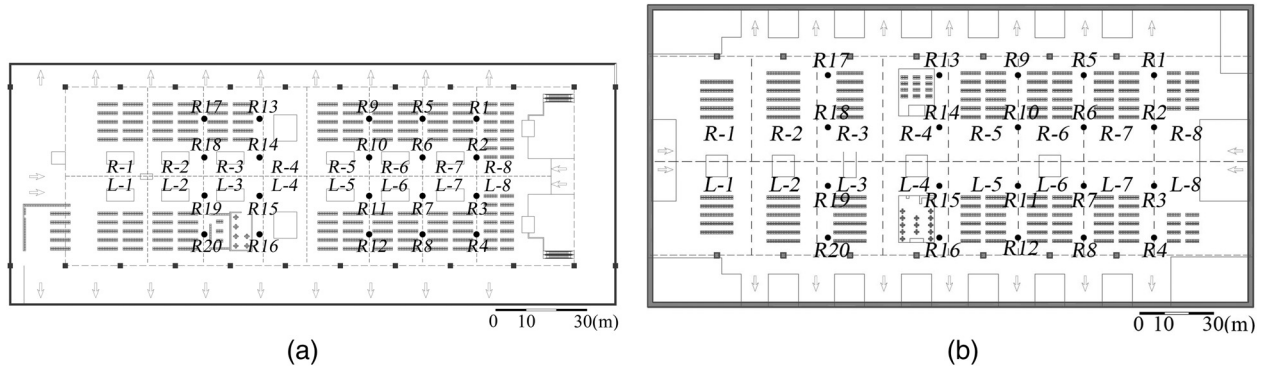


FIG. 6. The layout of measuring points in the waiting halls. SY, Shenyang station; CC, Changchun station. RNo. is the measuring point, the dotted lines showed the zoning, and L-No. or R-No. are the zoning numbers.

R9–R12; group 4, R13–R16; and group 5, R17–R20), and each group of 4 measuring points was cyclically tested by 1 tester. Each measuring point was measured for 1.5 min, and the test cycle lasted for 10 min;

- (b) the 1.5-min A-weighted equivalent noise level and 1-sec noise level were measured using AWA6228 Class-1 handheld sound level meters. The sound level meters were placed 1.5 m above the ground during the test; and
  - (c) each tester recorded the sound environment at the same time to rule out the impact of unexpected sudden noises, such as broadcast sounds based on the recordings and 1-s noise level.
- (2) Passenger and behavior count:
- (a) Number of passengers: The waiting hall is divided into 16 areas along the long side, as shown in Fig. 6. Area by area, photographs were taken on both sides of the seating area for the same period of 10 min to record the change in the number of passengers and spatial distribution of crowds during the test.
  - (b) Behavior: Video capture and observation were employed to analyze the crowd behavior.<sup>27</sup> Five randomly selected sites (SY R-2, 15:15–16:09; SY R-2, 16:40–17:58; CC, L-3 6:45–7:03; CC, L-4 7:30–8:41; CC, R-7 18:57–19:30) in Fig. 6 were videotaped on the second floor. The categories of behavior and behavior ratio in the survey locations were then counted from the review of videos in the laboratory. Only the passengers facing the camera were numbered and counted.

TABLE I. The main room information of the two waiting halls.

	Shenyang station	Changchun station
Length/width/height (m)	200/80/47.5	210/110/37
Floor area (m <sup>2</sup> )	16 000	23 100
Volume (m <sup>3</sup> )	760 000	854 700
Number of seats	2500	3650
Amount of annual passenger traffic (×10 <sup>6</sup> )	20.26	17.50

## IV. MEASUREMENT RESULTS

### A. Total noise level

Throughout the day, the mean noise level (see Fig. 7) changes in three stages: growth, fluctuation, and decline. The mean noise level at the Shenyang station varied between 58 and 71 dBA, while at Changchun station the mean noise level varied between 62 and 71 dBA. The mean noise level fluctuated significantly over short periods with a maximum variance of approximately 5 dBA within 10 min. It is worth noting that the rapid change in noise levels was caused by passengers as well as the broadcast.

### B. Crowd noise level and number of passengers

The changes in the crowd noise level and number of passengers are shown in Fig. 8. The crowd noise level was determined from the 1-s noise level data after excluding the broadcast times. The change in crowd noise level followed the same three-stage trend as did the change in overall noise level but was between 61 and 68 dBA, and the fluctuation over a short period of time was even lower, where the majority of the difference in noise level within 10 min is less than 1 dB.

The composition of crowds in the waiting halls is shown in Fig. 9 with the seating area consistently including most individuals, accounting for approximately 81.4%–95.8% of the total number of passengers, with an average of 87.7%. The number of passengers in the traffic area ranged from 4.2% to 18.7% of the total number of passengers with an average of 12.2%.

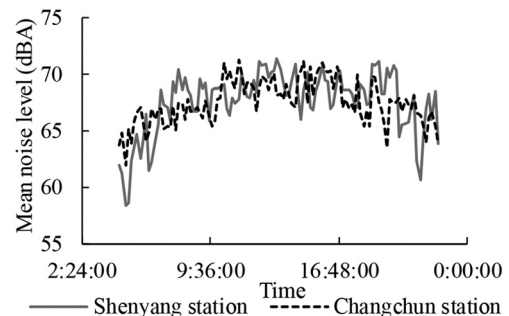


FIG. 7. The mean noise level.

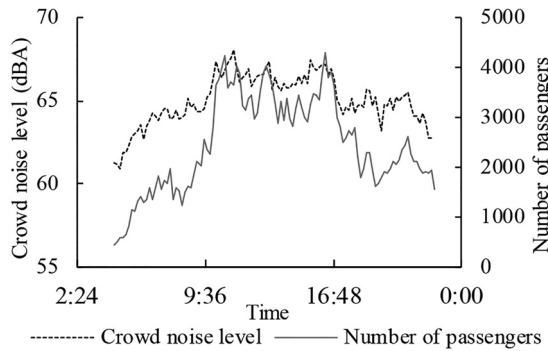


FIG. 8. The crowd noise level and number of passengers in Changchun station.

The number of passengers in each seating area throughout the day was also counted and used to calculate the average crowd spacing,  $m$ , in the seating area in Sec. VI using  $m = \sqrt{lw/N}$ , where  $l$  and  $w$  are the lengths of the seating area's long and short sides, respectively, and  $N$  is the number of passengers in that seating area. In Eq. (19), the number of passengers in the traffic area can be used directly.

**C. Behavior ratio**

The categories and counts of behaviors were determined according to five video recordings taken at various times in the two waiting halls. The behavior in each recording was counted every minute and averaged. As shown in Table II, the behavior can be roughly classified into two types: conversation (phone calls, two-person and three-person conversations) and footsteps (with or without luggage). Two-person conversations and footsteps without luggage dominated this behavior.

The relationship between the behavior ratio, total number of passengers, and time is shown in Fig. 10. The results showed that the behavior ratio at Shenyang station ranged from 10.34% to 45.45% with a mean value of approximately 24.58%. At Changchun station, the behavior ratio ranged from 10.34% to 52.27% with a mean value of approximately 28.80%. When crowd size and noise were small, the behavior ratio was more discrete but became more stable and less discrete as crowd size and noise increased, possibly resulting from the reduced desire for gossiping in the presence of high crowd size and background noise. Except for the CC R-6 area, the behavior ratio did not show a significant decrease

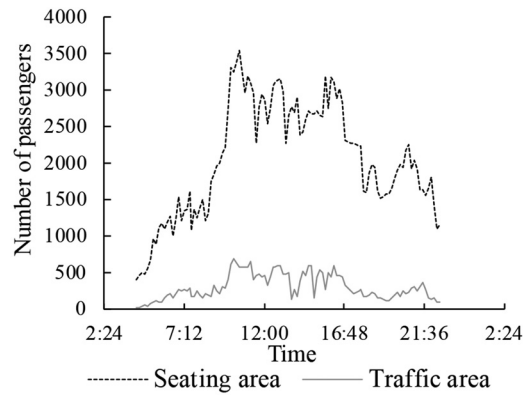


FIG. 9. The number of passengers in each functional area.

when crowd size and noise increased, which is in contrast to the change in the speaking ratio in the canteen.<sup>16</sup>

**D. Residual noise**

Long-term noise other than crowd noise and sudden noise, such as broadcast sounds, is referred to as residual noise<sup>18</sup> and usually comprises air conditioning noise, security check noise, gate noise, etc. (see Table III). Using the same method to measure the sound pressure level at 4:20 a.m. when the air conditioning and security lanes were on, the residual noise in the waiting room was found to be

$$SL_{\text{residual noise}} = SPL_{\text{measured crowd noise}} - SPL_{\text{Eq. (24)}}$$

**V. DETERMINATION OF AVERAGE CROWD SOUND POWER**

**A. Measurement and calculation of average crowd sound power**

A new approach for determining the average crowd sound power in a fixed area by measuring the noise in a localized area of a large space is proposed to avoid the problems of test environment distortion and overfitting of results as indicated in Sec. I. In a waiting hall, this fixed area corresponded naturally to a seating area, which was usually close to one of the ticket gates and, thus, generated a tidal change in crowds, that is, the number of passengers in this seating area decreased rapidly within a brief period of time prior to and following the start of check-in (mostly within 10 min) and then gradually increased until the next train arrived.

TABLE II. The behavior ratio in five test areas. SY, Shenyang Station; CC, Changchun Station.

Video	SY R-2 15:15-16:10	SY R-2 16:40-17:10	CC R-6 6:45-7:05	CC L-6 13:40-15:00	CC L-6 17:25-18:00	Mean
Total number of passengers	59	79	60	64	77	67.8
Phone call	2	1	1	1	0	1
Two-person conversation	4	7	7	4	8	6
Three-person conversation	2	1	1	0	1	1
Footstep	8	11	10	9	14	10.4
With luggage	1	1	2	2	3	1.8
Behavior ratio	27.12%	25.32%	31.67%	21.88%	29.87%	27.14%



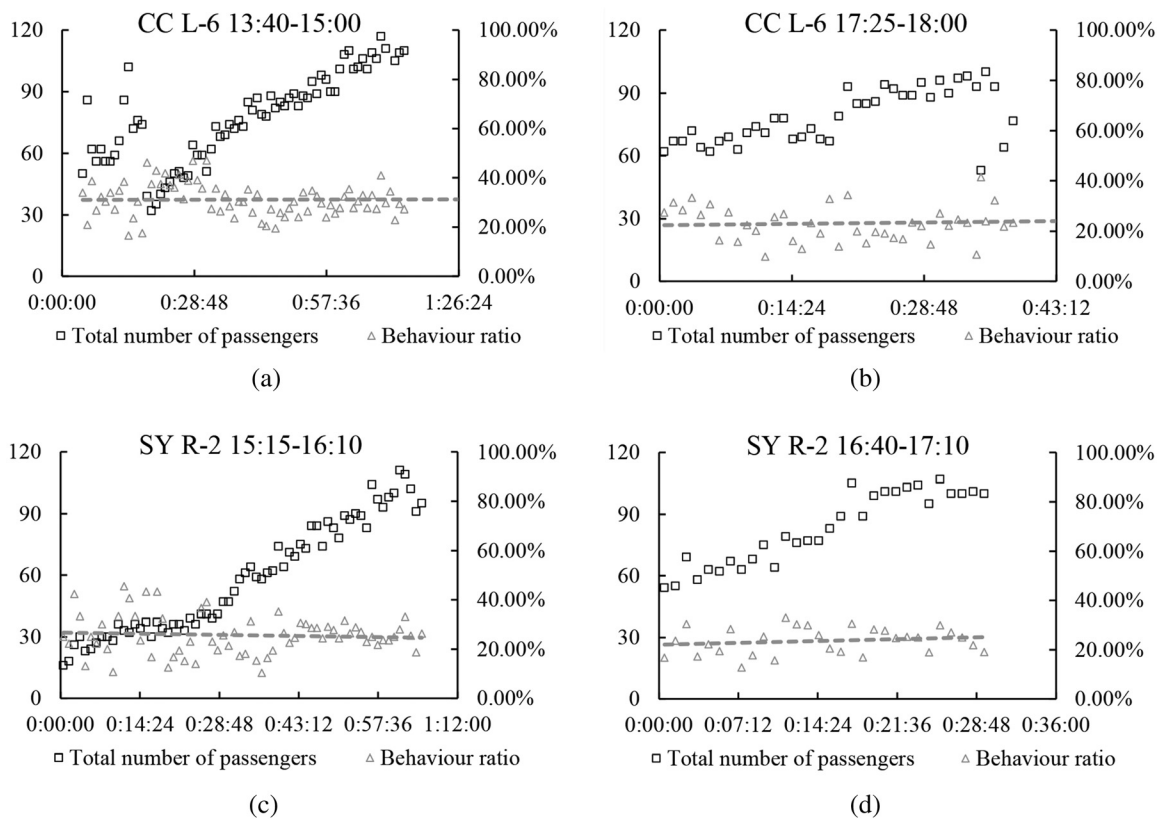


FIG. 10. The changes in behavior ratio with crowd size. SY, Shenyang station; CC, Changchun station.

The interior of the fixed area was considered a noise-generating area, and the rest of the area was considered the actual background environment. If the noise from the background environment is stable, as confirmed in Sec. IV B, the variation in noise at the receiver within the fixed area could be attributed entirely to short-term crowd tide variations, allowing for the calculation of the average crowd sound power within this seating area.

Furthermore, the reverberant sound energy generated by the noise sources might cause little variation in the noise at the receiver; therefore, the fixed seating area can be regarded as an approximate anechoic environment where only the superposition of the direct sound energy generated by the noise source needs to be taken into account when calculating the crowd sound power. This will be discussed later in this section.

Measurements were conducted to monitor changes in noise level and crowd numbers in the area prior to and following check-in.

- (a) A total of five areas where check-in was going to start were selected: 8:36–8:41, Changchun station L4; 8:55–9:05, Changchun station L5; 19:27–19:31, Changchun station R6; 16:48–16:54, Shenyang station L2; and 17:53–18:02, Shenyang station L2; and

- (b) the test indicators were the 1-s noise level and number of passengers: the sound level meter was placed in the center of the seating area, 1.5 m above the ground and 1.5 m distant from adjacent passengers; variations in the number of passengers were monitored via video on the second commercial floor.

The relationship between the change in crowd noise and number of passengers in the five areas is shown in Fig. 11. The changes in the number of passengers before and after check-in in the five areas were taken as 230 – 90, 120 – 60, 225 – 145, 220 – 110, and 160–50, and the corresponding changes in noise level were 64.7 – 61.3 dBA, 62.6 – 61.0 dBA, 63.6 – 61.5 dBA, 66.9 – 63.8 dBA, and 65.9 – 63.1 dBA, respectively, according to

$$L_p = 10 \lg(10^{L_1/10} + 10^{L_2/10} + \dots + 10^{L_n/10}). \quad (25)$$

The noise levels corresponding to crowd noise energy in the test area were 61.9, 57.5, 59.3, 64.0, and 62.7 dBA.

Given that the measuring point was in the center of the seating area, the sound pressure levels associated with crowd noise energy in the 1/4 seating area were 55.9, 51.5, 53.2, 58.0, and 56.7 dBA. The dimensions of the seating areas were measured as 19 × 18, 19 × 18, 19 × 18, 12 × 12, and 12 × 12 m<sup>2</sup>, and the crowd spacing was  $\sqrt{(19 \times 18)/140} = 1.56$  m,  $\sqrt{(19 \times 18)/60} = 2.35$  m,  $\sqrt{(19 \times 18)/80} = 2.07$  m,  $\sqrt{(12 \times 12)/110} = 1.14$  m, and  $\sqrt{(12 \times 12)/110} = 1.14$  m, respectively. Considering

TABLE III. The residual noise level of each receiver.

Receivers	R5	R6	R7	R8	R10	R11	R17	R18	R19	R20
Residual noise (dBA)	56.2	58.9	60.00	58.1	56.9	56.1	57.2	58.9	56.2	57.8

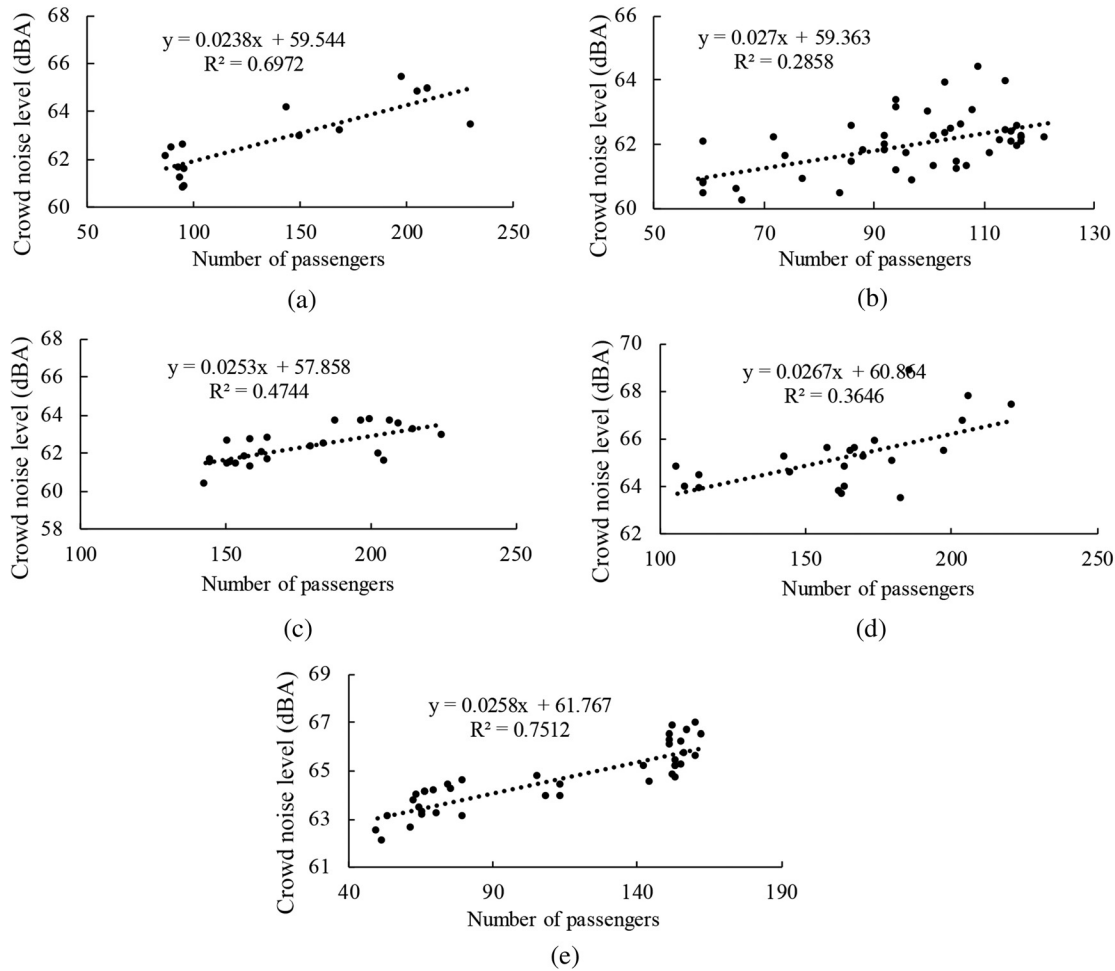


FIG. 11. The relationship between the crowd noise level and number of passengers in the check-in area.

solely direct sound energy, the individual’s average sound powers in the aforementioned five areas were 71.1, 70.1, 70.6, 71.1, and 70.0 dB with a mean value of 70.6 dB when using Eq. (14).

Considering direct and reverberant sound energy, the individual’s average sound powers in the aforementioned five areas were 70.9, 70.0, 70.4, 71.1, and 69.8 dB with a mean value of 70.4 dB as calculated using Eq. (18). Comparing the difference between the results of Eqs. (14) and (18), the variation in crowd noise attributable to the reverberant sound energy was only approximately 0.2 dB. Moreover, the reverberant sound level decreased more rapidly with distance in a non-diffuse field compared to a diffuse field;<sup>24,28</sup> therefore, the actual contribution of reverberant sound energy to the crowd level should be less than 0.2 dB. In summary, the reverberant sound energy can be ignored when calculating the crowd sound power.

**B. Lombard effect**

As background noise increases, crowds increase their voice output to maintain a suitable signal-to-noise ratio to sustain discourse, a phenomenon known as the Lombard effect.<sup>12,13</sup> Assuming a linear increase in the average speech

sound power after the background noise,  $L_N$ , exceeds 45 dBA,<sup>19,29,30</sup>

$$L_w = L_{w,Initial} + c(L_N - 45). \tag{26}$$

The Lombard slope,  $c$ , is influenced by factors such as the test environment and conditions, and Lazarus<sup>31</sup> showed that the Lombard slope ranged between around 0.5 and 0.7 dB/dB. The relationship between the average crowd sound power and background noise in a large waiting hall is shown in Fig. 12. The Lombard slope was approximately 0.18 dB/dB, which was lower than the empirical value of 0.5. It may be due to the fact that the average crowd sound power in this study reflected not only speech but also constant sound power behaviors, such as footsteps and luggage dragging, the result of the Lombard effect on average crowd sound power was relatively weaker.

**VI. VERIFICATION OF PREDICTION MODEL**

**A. Noise level in seating area**

Because all of the measuring points were located at the corner of the seating area and the circle simplification approach was only valid when the measuring point was

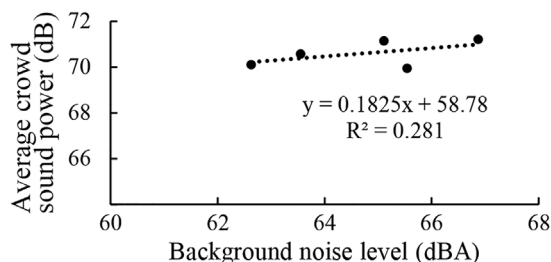


FIG. 12. The relationship between average crowd sound power and background noise.

located at the center of the seating area, the following calculations were performed using the square simplification method. The model input parameters are

- (1) Average crowd sound power,  $L_w$ : Background noise in the waiting hall was greater than 45 dBA throughout the day; therefore, the Lombard effect is always present.  $L_{w,Initial} = 70.6$  corresponds to a background noise of 64.7 dBA, thus, according to Eq. (26),

$$L_w = 70.6 + c(L_N - 64.7);$$

- (2) the crowd spacing,  $m$ , and number of passengers in each seating area are as illustrated in Sec. IV B; and
- (3) the behavior ratio = 27.1%.

According to Eqs. (14) and (18), the superpositions of sound energy of eight seating areas near the receiver were computed. For example, for the superposition of sound energy at receiver  $R5$ , the seating areas  $R-5-R-8$  and  $L-5-L-8$  were calculated while the crowd noise of the remaining seating areas was calculated using Eq. (21). The crowd noise level at receiver  $R5$  is  $SPL_{seating\ area} = SPL_{R-5} + \dots + SPL_{R-8} + SPL_{L-5} + \dots + SPL_{L-8} + SPL_{remaining}$ .

### B. Noise level in traffic area

To calculate the average absorption coefficient of the waiting hall, on-site surveys were conducted to determine the area and materials of the primary interior surfaces. The absorption coefficient of each material was extracted from the Odeon material library, and is presented in Table IV.

Based on the aforementioned data, the average absorption coefficient for 500–1000 Hz at Changchun station without passengers was calculated to be 0.22. Because passengers were heavily clothed during winter, the average absorption coefficient per passenger was considered to be 0.5.<sup>19</sup> Applying Eqs. (22) and (23) gave a reverberation radius of approximately 23.0 m at Changchun station. Approximately 4.6% of the traffic area was within the reverberation radius when the receiver was on both sides ( $R1, R4, R5, R8$ , etc.) and approximately 10.0% of the traffic area was within the reverberation radius when the receiver was in the center ( $R2, R3, R6, R7$ , etc.).

TABLE IV. The absorption coefficient of each material.

Material	Area (m <sup>2</sup> )	Absorption coefficient					
		125 Hz	250 Hz	500 Hz	1000 Hz	2000 Hz	4000 Hz
Marble slab	46 700	0.01	0.02	0.02	0.02	0.02	0.02
Glass window	10 600	0.35	0.25	0.8	0.12	0.07	0.04
Billboard	2400	0.12	0.12	0.3	0.48	0.66	0.66
Leather seat	4400	0.4	0.5	0.58	0.61	0.58	0.5
Grille ceiling	30 000	0.4	0.4	0.4	0.4	0.4	0.4
Open	1600	0.7	0.7	0.7	0.7	0.7	0.7
Air (4 M)		0	0	0	0.005	0.012	0.038

### C. Predicted and measured crowd noise level

The predicted crowd noise level at receiver  $R5$  was

$$SPL_{prediction} = SPL_{seating\ area} + SPL_{traffic\ area} + SPL_{residual\ noise}.$$

The predicted crowd noise level was calculated in the same way for the remaining receivers. Figure 13 shows a comparison between the on-site measured crowd noise and prediction results for the model using Eq. (14). The accuracy of the prediction model was evaluated using the  $R$ -square and the difference in crowd noise level between the predicted and measured results, as shown in Tables V and VI. The comparison results of receivers  $R1-R4, R9$ , and  $R12-R16$  were excluded because of partially missing on-site measurement data at these receivers.

The comparison and  $R$ -square of the predicted results for the model using Eq. (18), which contained the direct and reverberant sound energy of seating areas, are shown in Fig. 13 and Tables V and VI. The  $R$ -square of the model using Eq. (14) was consistently greater than that of the model using Eq. (18) for each receiver and average noise level. Moreover, the predicted results for the model using Eq. (18) were approximately 1 dB higher than those of the model using Eq. (14) and always tended to overestimate the measured results, which indicated that reverberant sound energy contributed negligibly to the noise level in a large waiting hall, presumably because of the predominance of ground reflections in extra-large spaces;<sup>2</sup> however, the presence of numerous obstructions on the floor blocked its reflection path.

Overall, the prediction model had relatively high accuracy in predicting the change trend of noise in the temporal and spatial dimensions with an  $R$ -square of approximately 0.5 for all of the receivers. However, the predicted noise levels of the model differed from the measured noise levels at some time points, especially when extreme values of measured noise levels were present, and the model tended to underestimate the changes in noise levels. In contrast, the model was considerably more accurate in predicting average crowd noise with an  $R$ -square of approximately 0.84. This might be due to the randomness of the behavior ratio and an individual's sound power, which makes it difficult to accurately predict crowd noise at a specific area by using an influencing factor with an average level. The relatively poor

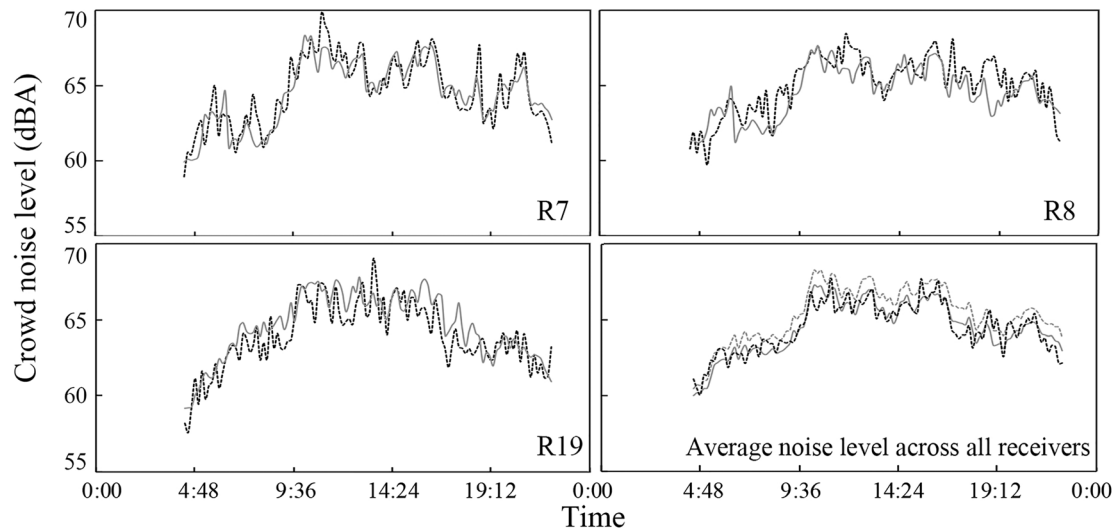


FIG. 13. The measured and predicted crowd noise levels in Changchun station, taking R7, R8, R19, and the average noise level across all of the receivers as examples. The measured noise level (black dashed line), predicted noise level using Eq. (14) (gray solid line), and predicted noise level using Eq. (18) (gray dashed line).

prediction accuracy at receiver R5 may be due to the proximity of R5 to the escalator.

Crowd noise levels were also calculated using the model proposed by Rindel and Hodgson with model input parameters based on on-site measurement results and recommended values from their study. The *R*-square of the model prediction results is shown in Table V. It can be seen that the prediction results were not satisfactory. This might be due to the fact that the model and input parameters were based on the assumption of a diffuse sound field. However, the parameters and accuracy of the model would vary depending on the spatial scale and the characteristics of the sound field.

#### D. Further research

There are a number of limitations to the work in this study. First, a prediction model was proposed based on a fixed location and large number of people in the seating area, which resulted in the model being applicable only to certain functionally extra-large spaces with fixed crowd locations. Second, because behavior ratios and crowd sound power are dynamic in temporal and spatial dimensions, the fixed values adopted in this study result in the model losing

its predictive accuracy at certain points in time. Finally, the model was verified solely in a Chinese waiting hall and further verification in an English-speaking environment is required.

#### VII. CONCLUSION

A crowd noise prediction model that accounts for the superposition of direct and reverberant sound energy was proposed, incorporating parameters such as spatial layout, seating area size, number and distribution of passengers, behavior ratio, and an individual’s average sound power.

To verify the prediction model, the above input parameters were measured in two typical waiting halls, as were the crowd noise levels throughout the day in one of the waiting halls. The crowd noise level changed between 61 and 68 dBA in an inverted trapezoidal trend during the entire operating period. The crowd noise level fluctuated slightly over a short period with the maximum difference in noise level being approximately 1.4 dBA within 10 min. The behavior ratio fluctuated considerably, ranging between approximately 10% and 50% with an average value of approximately 27.1%, and was dominated by two-person conversations and footsteps without luggage.

TABLE V. The *R*-square of the prediction model. ANL is the average noise level across all of the receivers.

Receivers	R5	R6	R7	R8	R10	R11	R17	R18	R19	R20	ANL
Eq. (14)	0.28	0.52	0.77	0.56	0.51	0.57	0.41	0.55	0.67	0.39	0.84
Eq. (18)	0.45	0.19	0.66	0.61	0.09	0.14	0.14	0.05	0.27	0.36	0.51
Rindel						-7.84					
Hodgson						0.36					

TABLE VI. The difference in crowd noise level between predicted results and measured results. The average and maximum of the difference in crowd noise levels are shown. ANL is the average noise level across all of the receivers.

	Difference (dBA)	Receivers										ANL
		R5	R6	R7	R8	R10	R11	R17	R18	R19	R20	
Eq. (14)	Average	1.64	1.17	0.86	0.96	1.15	1.05	1.03	1.00	1.00	1.45	0.53
	Maximum	6.12	3.18	3.27	3.87	3.56	3.84	3.00	3.25	2.87	4.88	1.69
Eq. (18)	Average	1.49	1.79	1.23	1.05	1.82	1.77	1.34	1.80	1.78	1.53	0.98
	Maximum	4.53	4.18	2.78	3.04	4.75	4.38	4.35	4.51	3.79	4.23	2.48

The individual’s average sound power was determined by the measurement method proposed in this study, which was based on the rapid change in the number of crowds and noise levels in a fixed seating area within a brief period of time prior to and following the start of the check-in. The results of the measurements and calculations for the five seating areas indicated that the average sound power was approximately 70.6 dB.

Finally, the model was verified using the measured data and further discussion ensued regarding whether the model should include the reverberant sound energy. The results showed that the model that considered only direct sound energy in the seating area was capable of accurately predicting the average crowd noise in large waiting halls, whereas for the fluctuations of crowd noise in the temporal and spatial dimensions, the model could accurately predict the change trend but tended to underestimate the level of change, and the model that included reverberant sound energy tended to overestimate the crowd noise level.

**ACKNOWLEDGMENTS**

This work was supported by the National Natural Science Foundation of China (Grant No. 51978454) and the second batch of 2021 Ministry of Education of the People’s Republic of China Industry-University Collaborative Education Program, Kingfar-Chinese Ergonomics Society “Human Factors and Ergonomics” Program (Grant No. 202102055010).

<sup>1</sup>TB 10100-2018, *Code for Design of Railway Passenger Station* (State Railway Administration, Beijing, 2018).  
<sup>2</sup>C. Wang, H. Ma, Y. Wu, and J. Kang, “Characteristics and prediction of sound level in extra-large spaces,” *Appl. Acoust.* **134**, 1–7 (2018).  
<sup>3</sup>Y. Wu, J. Kang, W. Zheng, and Y. X. Wu, “Acoustic comfort in large railway stations,” *Appl. Acoust.* **160**, 107137 (2020).  
<sup>4</sup>P. J. Liu, “Investigation of noise conditions in waiting halls of high-speed railway stations,” *Noise Vib. Control* **38**(3), 120–123 (2018) (in Chinese).  
<sup>5</sup>H. S. Liu, H. Ma, J. Kang, and C. Wang, “The speech intelligibility and applicability of the speech transmission index in large spaces,” *Appl. Acoust.* **167**, 107400 (2020).  
<sup>6</sup>M. J. Hayne, R. H. Rumble, and D. J. Mee, “Prediction of crowd noise,” in *Proceedings of Acoustics*, Christchurch, New Zealand (2006), pp. 235–240.  
<sup>7</sup>T. T. Yang, F. Aletta, and J. Kang, “Sound environments in large public buildings for crowd transit: A systematic review,” *Appl. Sci.* **11**(9), 3728 (2021).  
<sup>8</sup>Q. Meng, T. Z. Gong, and Y. S. Du, “Evaluation of sound environment in the waiting halls of railway stations,” *Adv. Mater. Res.* **518-523**, 3809–3813 (2012).  
<sup>9</sup>J. Chen and H. Ma, “An impact study of acoustic environment on users in large interior spaces,” *Build. Acoust.* **26**(2), 139–153 (2019).

<sup>10</sup>X. H. Du, Y. C. Zhang, and S. J. Zhao, “Research on interaction effect of thermal, light and acoustic environment on human comfort in waiting hall of high-speed railway station,” *Build. Environ.* **207**, 108494 (2022).  
<sup>11</sup>I. R. Cushing, F. F. Li, T. J. Cox, K. Worrall, and T. Jackson, “Vocal effort levels in anechoic conditions,” *Appl. Acoust.* **72**(9), 695–701 (2011).  
<sup>12</sup>H. L. Pick, Jr., G. M. Siegel, P. W. Fox, S. R. Garber, and J. K. Kearney, “Inhibiting the Lombard effect,” *J. Acoust. Soc. Am.* **85**(2), 894–900 (1989).  
<sup>13</sup>J. C. Junqua, “The Lombard reflex and its role on human listeners and automatic speech recognizers,” *J. Acoust. Soc. Am.* **93**(1), 510–524 (1993).  
<sup>14</sup>M. J. Hayne, J. C. Taylor, R. H. Rumble, and D. J. Mee, “Prediction of noise from small to medium sized crowds,” in *Proceedings of Acoustics*, Gold Coast, Australia (2011).  
<sup>15</sup>M. Hodgson, G. Steininger, and Z. Razavi, “Measurement and prediction of speech and noise levels and the Lombard effect in eating establishments,” *J. Acoust. Soc. Am.* **121**(4), 2023–2033 (2007).  
<sup>16</sup>C. Wang, X. J. Kong, S. Yao, J. Kang, and J. Y. Yuan, “Crowd noise and vocal power level in large college canteens in China,” *Appl. Acoust.* **182**, 108242 (2021).  
<sup>17</sup>M. Hodgson, R. Rempel, and S. Kennedy, “Measurement and prediction of typical speech and background-noise levels in university classrooms during lectures,” *J. Acoust. Soc. Am.* **105**(1), 226–233 (1999).  
<sup>18</sup>M. P. N. Navarro and R. L. Pimentel, “Speech interference in food courts of shopping centres,” *Appl. Acoust.* **68**(3), 364–375 (2007).  
<sup>19</sup>J. H. Rindel, “Verbal communication and noise in eating establishments,” *Appl. Acoust.* **71**(12), 1156–1161 (2010).  
<sup>20</sup>J. H. Rindel, “Restaurant acoustics—Verbal communication in eating establishments,” *Acoust. Pract.* **7**(1), 1–14 (2019).  
<sup>21</sup>W. K. Connor, “On the noise of crowds,” *J. Acoust. Soc. Am.* **41**(6), 1590 (1967).  
<sup>22</sup>L. Nijs, K. Saher, and D. den Ouden, “Effect of room absorption on human vocal output in multitalker situations,” *J. Acoust. Soc. Am.* **123**(2), 803–813 (2008).  
<sup>23</sup>M. Hodgson, “Experimental evaluation of the accuracy of the Sabine and Eyring theories in the case of non-low surface absorption,” *J. Acoust. Soc. Am.* **94**(2), 835–840 (1993).  
<sup>24</sup>M. Hodgson, “When is diffuse-field theory applicable,” *Appl. Acoust.* **49**(3), 197–207 (1996).  
<sup>25</sup>S. K. Tang, D. W. Chan, and K. C. Chan, “Prediction of sound-pressure level in an occupied enclosure,” *J. Acoust. Soc. Am.* **101**(5), 2990–2993 (1997).  
<sup>26</sup>J. Kang, “Numerical modelling of the speech intelligibility in dining spaces,” *Appl. Acoust.* **63**(12), 1315–1333 (2002).  
<sup>27</sup>Q. Meng and J. Kang, “Effect of sound-related activities on human behaviours and acoustic comfort in urban open spaces,” *Sci. Total Environ.* **573**, 481–493 (2016).  
<sup>28</sup>M. Barron, “Theory and measurement of early, late and total sound levels in rooms,” *J. Acoust. Soc. Am.* **137**(6), 3087–3098 (2015).  
<sup>29</sup>T. S. Korn, “Effect of psychological feedback on conversational noise reduction in rooms,” *J. Acoust. Soc. Am.* **26**(5), 793–795 (1954).  
<sup>30</sup>P. Bottalico, I. I. Passione, S. Graetzer, and E. J. Hunter, “Evaluation of the starting point of the Lombard effect,” *Acta Acust. Acust.* **103**(1), 169–172 (2017).  
<sup>31</sup>H. Lazarus, “Prediction of verbal communication is noise—A review: Part 1,” *Appl. Acoust.* **19**(6), 439–464 (1986).